REFERENCES AND NOTES

1. J. B. Lambert *et al.*, *Science* **260**, 1917 (1993).
2. K. Shelly, D. C. Finster, Y. J. Lee, W. R. Scheidt, C. A. Reed, *J. Am. Chem. Soc.* **107**, 5955 (1985).
3. J. Vicente, M. T. Chicote, I. Saura-Llamas, *Organometallics* **8**, 767 (1989).
4. W. S. Sheldrick, *The Chemistry of Organic Silicon Compounds*, S. Patai and Z. Rappoport, Eds. (Wiley, New York, 1989), part 1, p. 246.
5. Z. Xie *et al.*, *J. Chem. Soc. Chem. Commun.* **1993**, 384 (1993).
6. J. Haggin, *Chem. Eng. News* **71** (no. 26), 7 (1993).
7. N. C. Baenziger and A. D. Nelson, *J. Am. Chem. Soc.* **90**, 6602 (1968).
8. M. Kira *et al.*, *Chem. Lett.* **1993**, 153 (1993).
9. S. R. Bahr and P. Boudjouk, *J. Am. Chem. Soc.* **115**, 4514 (1993).
10. G. K. S. Prakash *et al.*, *ibid.* **109**, 5123 (1987).
11. J. B. Lambert and S. Zhang, *J. Chem. Soc. Chem. Commun.* **1993**, 383 (1993).
12. Z. Xie, T. Jelínek, R. Bau, C. A. Reed, unpublished results.
13. *i*-Pr_3SiH (20.1 mg, 0.127 mmol) was added to a suspension of $[Ph_3C^+][Br_6\text{-}CB_{11}H_6^-]$ (60.0 mg, 0.0698 mmol) in dry toluene (25 ml). The mixture was stirred at room temperature overnight to give a pale-yellow solution. *n*-Hexane vapor diffusion resulted in colorless crystals (35.5 mg, 66%). ^{11}B NMR (C_6D_6): −1.43 (s, 1B), −9.69 (s, 5B), and −20.06 (d, 5B). Elemental analysis: calculated for $C_{10}H_{27}B_{11}Br_6Si$, C, 15.52% and H, 3.52%; found, C, 15.59% and H, 3.57%.
14. The structure was solved by direct methods. Triclinic *P*1(bar), with unit cell parameters a = 11.124(8), b = 15.628(15), c = 8.000(9)Å, α = 94.96(8), β = 98.85(8), γ = 76.30(7)°, V = 1333(2) Å^3 for Z = 2 (errors in last digits in parentheses). Final factor R = 6.37% for 1296 reflections with $I > 3\sigma(I)$.
15. M. D. Harmony and M. R. Strand, *J. Mol. Spectrosc.* **81**, 308 (1980).
16. X. Yang, C. L. Stern, T. J. Marks, *Organometallics* **10**, 840 (1991).
17. S. D. Grumbine, T. D. Tilley, F. P. Arnold, A. L. Rheingold, *J. Am. Chem. Soc.*, in press.

18. Supported by the National Science Foundation (grants CHE 89-17888 and CHE 92-23260).

22 July 1993; accepted 3 September 1993

Production of Perfluoroalkylated Nanospheres from Buckminsterfullerene

Paul J. Fagan,* Paul J. Krusic,* C. N. McEwen, J. Lazar, Deborah Holmes Parker,† N. Herron, E. Wasserman

Perfluoroalkylated nanospheres have been prepared by reaction of fullerenes with a variety of fluoroalkyl radicals. The latter are generated by thermal or photochemical decomposition of fluoroalkyl iodides or fluorodiacyl peroxides. Up to 16 radicals add to C_{60} to afford easily isolable fluoroalkylated derivatives. The monosubstituted radical adducts were detected by electron spin resonance in the early stages of the fluoroalkylation reactions. These spheroidal molecules are thermally quite stable, soluble in fluoroorganic solvents, chemically resistant to corrosive aqueous solutions, and more volatile than the parent fullerenes. Films of the sublimed material display properties typical for a perfluoroalkylated material.

Since the discovery of the large-scale synthesis of C_{60} (*1*), the fluorination of this molecule and the properties of $C_{60}F_n$ materials have aroused keen interest (*2*). There was the potential that unique, chemically resistant "fluorinated balls" would result that might have interesting physical properties (*3*). However, $C_{60}F_n$ compounds are unstable with respect to hydrolysis and readily lose fluoride ions, generating HF (*4*). We reasoned that perfluoroalkylation of C_{60} might provide the necessary stability against hydrolysis yet present a chemically resistant, fluorinated, hydrophobic surface to the external environment (*5*). High thermal stability might be expected for such materials because both perfluoroalkanes and C_{60} are exceptionally thermally stable.

Central Research and Development Department, E. I. du Pont de Nemours & Company, Experimental Station, P.O. Box 80328, Wilmington, DE 19880–0328.

*To whom correspondence should be addressed.
†Present address: Procter and Gamble Company, Sharon Woods Technical Center, Cincinnati, OH 45241–9974.

We prepared such perfluoroalkylated nanospheres by adding perfluoroalkyl free radicals to C_{60}. These are generated by thermal or photochemical decomposition of radical precursors such as fluoroalkyl iodides, R_fI, and fluorodiacyl peroxides, $R_f\text{-}C(O)O\text{-}O(O)C\text{-}R_f$. We also report the electron spin resonance (ESR) detection of the radical species $R_f\text{-}C_{60}^{\cdot}$ formed in the early stages of these reactions by addition of a single fluoroalkyl radical to C_{60}. The behavior of these reaction intermediates is similar to that recently delineated for their hydrocarbon analogs (*6*). This similarity includes the tendency to form weakly bonded, dumbbell-shaped dimers $R_f\text{-}C_{60}\text{-}C_{60}\text{-}R_f$ for which the dimer bond strength can be determined by ESR (*7*).

Heating C_{60} and excess perfluorohexyl iodide in 1,2,4-trichlorobenzene at 200°C with exclusion of oxygen produced after work-up a dark-brown glassy solid for which elemental analysis afforded the formula $C_{60}[(CF_2)_5CF_3]_{9.5}H_2$ (*8*). The electron-capture mass spectrum of this sample (*9*), facilitated by the remarkable volatility of the material, showed the addition of 6 to 12 perfluorohexyl groups to C_{60} (Fig. 1A). Although the relative intensity distribution varied somewhat for scans taken at different probe temperatures, the most intense peak always corresponded to 10 perfluorohexyl addends, consistent with the elemental analysis.

From ^{13}C nuclear magnetic resonance (NMR) spectra, evidence was obtained for an average of 8 to 10 perfluoroalkyl groups on each C_{60}. A broad resonance from 160 to 130 parts per million (ppm) was attributed to unreacted C=C double bonds on C_{60}; broad and sharp resonances from 125 to 105 ppm were assigned to perfluoroalkyl-group carbon resonances; finally, a broad resonance centered at 62 ppm was attributed to C_{60} carbons bearing perfluoroalkyl groups. The ratio of the intensity of this last resonance to that of the broad resonance between 160 and 130 ppm was about 6:1, appropriate for an average of 8 to 10 perfluoroalkyl substituents on each C_{60}. A very small extent of hydrogen incorporation was indicated by the expansion of each mass spectral peak. The expanded peak corresponding to C_{60} with 10 perfluorohexyl groups was simulated as a mixture of $C_{60}(R_f)_{10}^-$, $C_{60}(R_f)_{10}H^-$, $C_{60}(R_f)_{10}H_2^-$, $C_{60}(R_f)_{10}H_3^-$, and $C_{60}(R_f)_{10}H_4^-$ in the ratios 1.0:0.78:1.0:0.78:0.11 (Fig. 1A, inset). Consistent with this finding, ^1H NMR did show a broad resonance from 5.5 to 3.8 ppm, which we attribute to hydrogens on the C_{60} sphere. The ^{19}F NMR was more informative with resonances in the CF_2 chemical shift region and a single resonance in the CF_3 region (*10*).

Substantial coverage of C_{60} with fluoroalkyl groups can also be achieved at room temperature by photolysis of perfluoroalkyl iodides. For example, a saturated benzene solution of C_{60} with excess trifluoromethyl iodide was irradiated with ultraviolet light in a sealed quartz tube for 30 min. Electron-capture mass spectrometry showed addition of up to 13 CF_3 groups to C_{60} (Fig. 2A). Unlike the relative sharpness of the mass spectrum discussed above, each CF_3 adduct showed up as a cluster of masses, as wide as 30 mass units, indicating substantial hydrogen atom incorporation that progressively increased with the number of CF_3 groups. Negative-ion Fourier transform mass spectra (FTMS), expanded in the mass region appropriate for the addition of two and three CF_3 groups, peaked at compositions corresponding to $C_{60}(CF_3)_2H_3^-$ and $C_{60}(CF_3)_3H_4^-$ (Fig. 2A, inset). The peaks of all mass clusters were appropriately shifted toward higher masses when perdeuteriobenzene was used as the solvent. The hydrogen transfer from benzene most likely occurs in two steps: addition of $CF_3^{\cdot}$ radicals to benzene to yield a CF_3-substi-

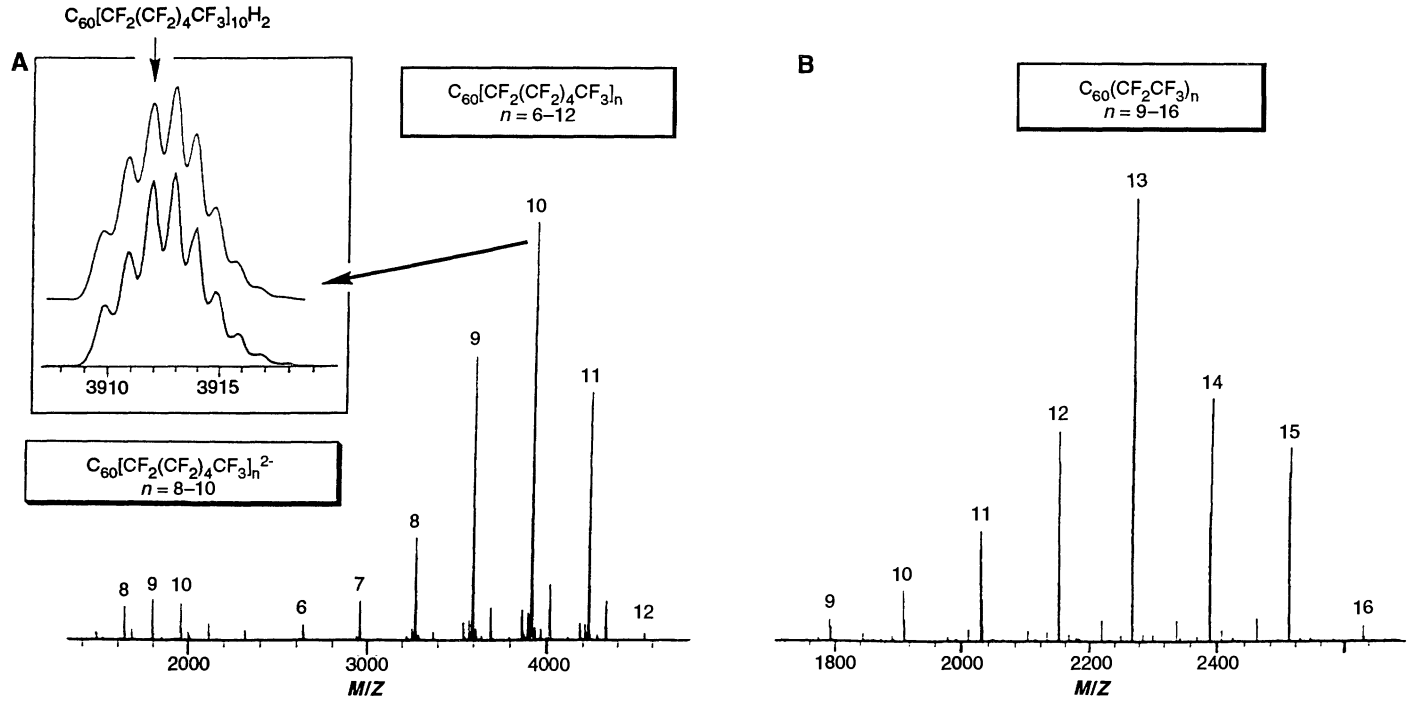

Fig. 1. Electron-capture mass spectra of the products obtained by reaction of C_{60} with (**A**) perfluorohexyl iodide in 1,2,4-trichlorobenzene at 175°C and (**B**) perfluoropropionyl peroxide in Freon 113 at 25°C showing the addition of perfluorohexyl and perfluoroethyl radicals to C_{60}. (**Inset**) The high-resolution scan of the peak corresponding to C_{60} with 10 perfluorohexyl groups (lower curve) can be simulated (upper curve) on the basis of the expected ^{13}C isotopomers and assuming incorporation of one to four hydrogen atoms.

tuted cyclohexadienyl radical (*11*) that subsequently transfers a hydrogen atom to a $C_{60}(CF_3)_nH_m$ species (*12*, *13*).

To avoid hydrogen incorporation altogether, and bearing in mind the remarkable solubility of $C_{60}(R_f)_n$ in fluoroorganic solvents, it seemed reasonable to carry out the radical reactions in a fluorocarbon or in a halofluorocarbon, notwithstanding the essential insolubility of C_{60} in such media. Indeed, heating an initially heterogeneous mixture of C_{60} and excess trifluoromethyl iodide in hexafluorobenzene at 200°C for 24 hours in a sealed glass tube led to a dark red-brown solution. The electron-capture mass spectrum showed sharp peaks corresponding to the clean addition of up to 14 CF_3 groups to C_{60} (Fig. 2B). Similar results were obtained with perfluoroethyl, perfluoropropyl, and perfluorohexyl iodides.

Other sources of fluoroalkyl radicals can also be used. Reaction of C_{60} with a ~6% Freon 113 solution of perfluoropropionyl peroxide, C_2F_5-C(O)O-O(O)C-C_2F_5, at 25°C produced clear dark-brown solutions. A typical electron-capture mass spectrum of the product showed from 9 to 16 perfluoroethyl groups attached to C_{60} (Fig. 1B). A similar number of perfluoroethyl radicals also add to C_{70} under analogous conditions, indicating that fluoroalkyl radicals will add readily to other fullerenes.

The solid perfluorohexylated material appeared amorphous by high-resolution

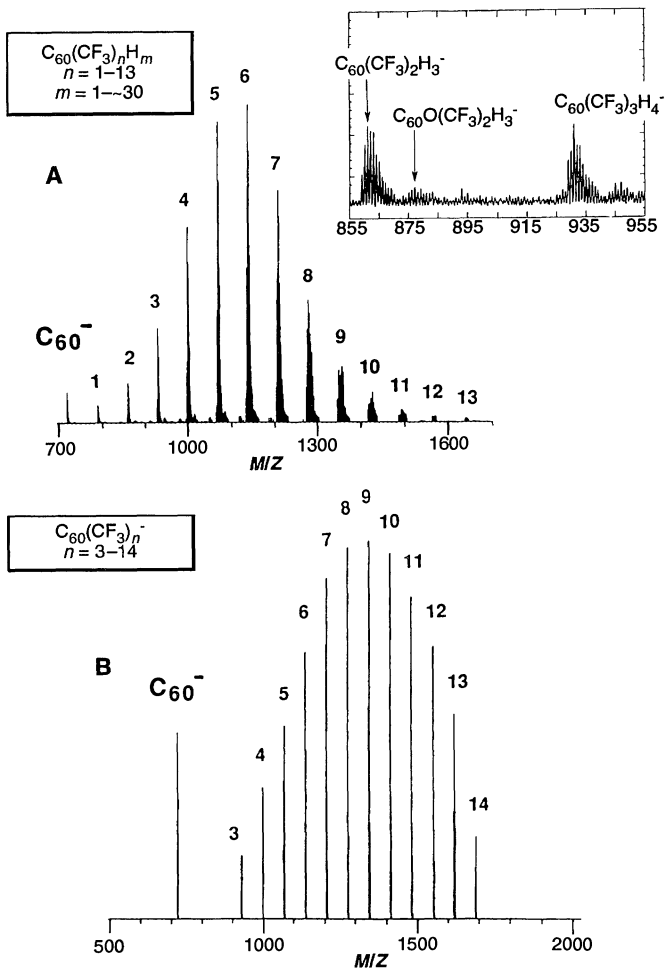

Fig. 2. Electron-capture mass spectra of the products obtained (**A**) by ultraviolet irradiation of C_{60} in benzene containing iodotrifluoromethane at 25°C and (**B**) by heating an initially heterogeneous mixture of C_{60} and excess iodotrifluoromethane in hexafluorobenzene at 200°C showing the addition of CF_3 radicals to C_{60}. The photochemical reaction in benzene leads to substantial hydrogenation of the CF_3 derivatives of C_{60}, as illustrated by (**inset**) the negative-ion FTMS spectrum. Insignificant oxygen incorporation is noticed only by FTMS of samples exposed to air and is attributed to the effects of laser desorption in the mass spectrometer.

electron microscopy, and no electron diffraction was observed. Thermal gravimetric analysis (TGA) under flowing helium showed a weight loss beginning at 270°C with complete (residual ≤ 2%) weight loss occurring at ~400°C. The major source of weight loss was sublimation of the material, as confirmed by mass spectrometry. In air, the TGA curve was identical to that under helium but began to tail at ~350°C, and complete weight loss did not occur until 550°C. Differential scanning calorimetry revealed no obvious phase transitions (up to 280°C) as might be expected for a noncrystalline substance. We conclude that the material is thermally stable to at least 270°C and is much more volatile than the parent fullerene. Under high vacuum, the perfluorohexylated nanospheres can be sublimed quantitatively to deposit a thin film on a glass slide. Advancing and receding contact angles were determined for this film with both water (124° ± 3° and 64° ± 3°, respectively) and hexadecane (65° ± 3° and 24° ± 3°, respectively). These numbers are in the range observed for other perfluoroalkylated surfaces (*14*). No chemical changes were observed upon treatment of the film with aqueous sulfuric acid or sodium hydroxide.

The involvement of free radical intermediates in these reactions can be easily established by ESR. Heating 1,2,4-trichlorobenzene solutions of C_{60} containing perfluorohexyl iodide above 400 K in the cavity of the spectrometer afforded the spectrum of the first-formed radical adduct $CF_3(CF_2)_5$-$C_{60}^{\cdot}$ (Fig. 3A). The splitting pattern (triplet of triplets of triplets) is diagnostic of three pairs of interacting CF_2 fluorines. The splittings of 0.52, 2.63, and 0.10 G at 400 K can be assigned to the first three pairs, counting from the C_{60} surface, by analogy with CF_3CF_2-$C_{60}^{\cdot}$ (Fig. 3B). The latter was obtained by heating above 400 K a saturated *tert*-butylbenzene solution of C_{60} containing either one to two equivalents of perfluoropropionyl peroxide or a small molar excess of CF_3CF_2I. The spectrum consisted of a quartet of triplets for three equivalent CF_3 and two equivalent CF_2 fluorines (2.29 and 0.50 G, respectively, at 420 K). Thus, the larger splitting is clearly associated with the fluorines of the second carbon in the fluoroalkyl chain.

The ESR data collectively indicate the following: (i) The rotation about the bond connecting the fluoroalkyl group to C_{60} is strongly hindered. The equivalence of the fluorines on the CF_2 group closest to the C_{60} surface in perfluoro-*n*-alkyl radical adducts requires a symmetric equilibrium conformation (illustrated below) for the perfluoroethyl adduct (*15*).

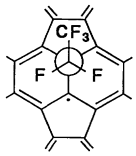

(ii) The temperature-dependent broadening of the central triplet of triplets in Fig. 3A, observed also for other perfluoro-*n*-alkyl adducts of C_{60}, precludes the symmetric *trans* equilibrium conformation (Fig. 4C). Instead, the two fluorines on C-8 are exchanging between two inequivalent sites at insufficient rates for dynamic equivalence on the ESR time scale (~1 μs) (*16*). Equivalence would result in 1:2:1 relative intensities for the triplet with the largest splitting (Fig. 3A). Such inequivalent sites, a and b, arise naturally in a *gauche* (Fig. 4A) or a twist-*anti* equilibrium conformation (Fig. 4B). We favor the latter, which is similar to the arrangement of vicinal CF_2 units in the helical structure of polytetrafluoroethylene (twist angle of ~13°) (*17*). (iii) The reversible temperature dependence of the ESR intensity for the perfluoroethyl adduct (Fig. 3, inset) indicates that above ~400 K, this radical is in equilibrium with a diamagnetic dimer in complete analogy with the hydrocarbon analogs (6).

Finally, we point out that the number of perfluoroalkyl groups needed to effectively cover the C_{60} surface with a fluorocarbon coating is not large. An upper limit below 24 is suggested by the highly symmetric structure of $C_{60}Br_{24}$ (*18*) because we have not been able to assemble $C_{60}(CF_3)_{24}$ by computer modeling using the structural parameters of this brominated derivative without unrealistic steric crowding (*19*).

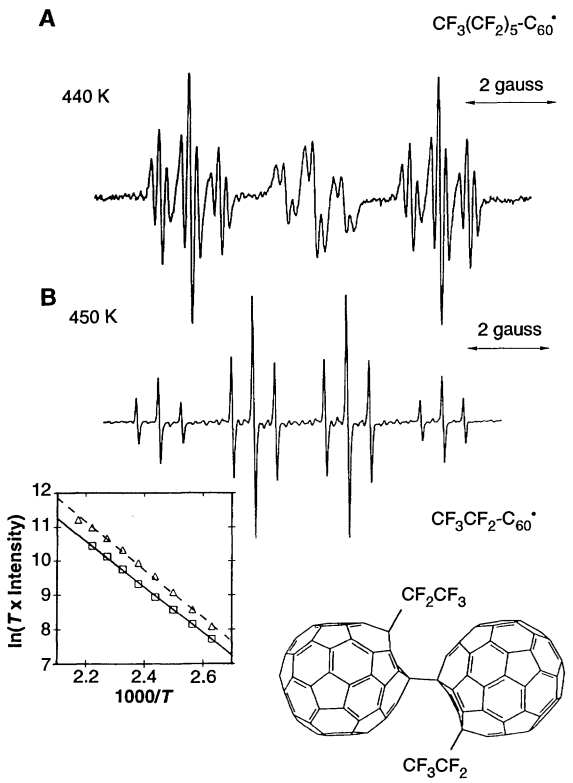

Fig. 3. The ESR spectra of the radicals formed by addition to C_{60} of (**A**) a single perfluorohexyl radical (solvent, 1,2,4-trichlorobenzene) and (**B**) a perfluoroethyl radical (solvent, *tert*-butylbenzene). (**Inset**) Temperature dependence of the ESR intensity for the CF_3CF_2-$C_{60}^{\cdot}$ adduct generated with perfluoroethyl iodide (squares) and perfluoropropionyl peroxide (triangles). The slope gives −26.6 kcal/mol for the enthalpy change accompanying dimer dissociation and therefore for the dimer bond strength. Also shown is a molecular model of the dimer resulting by the coupling of two CF_3CF_2-$C_{60}^{\cdot}$ radicals at carbons 3 or 3′ (see Fig. 4A for the numbering of carbon atoms) as established for the hydrocarbon analogs (*6, 20*).

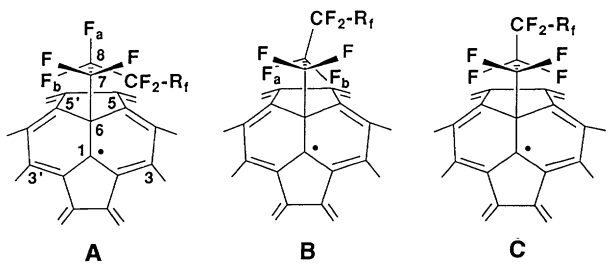

Fig. 4. Structures showing the numbering of the carbon atoms and the sites, a and b, of the (**A**) *gauche*, (**B**) twist-*anti*, and (**C**) symmetric *trans* equilibrium conformations.

REFERENCES AND NOTES

1. W. Krätschmer *et al.*, *Nature* **347**, 354 (1990); R. Taylor *et al.*, *Chem. Commun.* **1990**, 1423 (1990); H. Ajie *et al.*, *J. Phys. Chem.* **94**, 8630 (1990); R. E. Haufler *et al.*, *ibid.*, p. 8634.
2. J. H. Holloway *et al.*, *Chem. Commun.* **1991**, 966 (1991); H. Selig *et al.*, *J. Am. Chem. Soc.* **113**,

5475 (1991); R. Taylor *et al.*, *Chem. Commun.* **1992**, 665 (1992); A. A. Tuinman *et al.*, *J. Phys. Chem.* **96**, 7584 (1992); I. Belaish *et al.*, *Adv. Mater.* **4**, 411 (1992); T. Nakajima and Y. Matsuo, *Carbon* **30**, 1119 (1992); P. J. Benning *et al.*, *Phys. Rev. B* **47**, 1589 (1993); A. A. Tuinman *et al.*, *J. Am. Chem. Soc.* **115**, 5885 (1993); K. Kniaz *et al.*, *ibid.*, p. 6060.
3. R. F. Curl and R. E. Smalley, *Sci. Am.*, 62 (October 1991).
4. R. Taylor *et al.*, *Nature* **355**, 27 (1992).
5. These spheroidal molecules can be thought of as nanospheres covalently bonded to small oligomers of tetrafluoroethylene, the principal component of Teflon (a registered trademark for fluoropolymer resins, films, and fibers made by DuPont).
6. P. J. Krusic *et al.*, *J. Am. Chem. Soc.* **113**, 6274 (1991); P. J. Krusic, E. Wasserman, P. N. Keizer, J. R. Morton, K. F. Preston, *Science* **254**, 1183 (1991); J. R. Morton *et al.*, *J. Phys. Chem.* **96**, 3576 (1992); J. R. Morton *et al.*, *J. Chem. Soc. Perkin Trans. 2* **1992**, 1425 (1992); P. J. Krusic *et al.*, *J. Phys. Chem.* **97**, 1736 (1993); J. R. Morton *et al.*, *Chem. Phys. Lett.* **204**, 481 (1993); P. N. Keizer *et al.*, *J. Chem. Soc. Perkin Trans. 2* **1993**, 1041 (1993).
7. J. R. Morton *et al.*, *J. Am. Chem. Soc.* **114**, 5454 (1992).
8. Heating C_{60} (300 mg) in a sealed vessel with perfluorohexyl iodide (6 ml) in 1,2,4-trichlorobenzene (15 ml) for 24 hours at 175°C under 5 to 20 psi of nitrogen produced dark red-brown reaction mixtures. The characteristic color of iodine vapor could be seen in the glass vessel during reaction. The residue obtained after removal of the solvent by distillation (10^{-4} torr) was highly soluble in hexafluorobenzene and $CClF_2CCl_2F$ (Freon 113), in sharp contrast with the total insolubility of C_{60} in these solvents, and was filtered from any remaining solids. It was purified by two precipitations from Freon 113 solutions with dichloromethane to yield a glassy solid when dried (1.35 g). A typical elemental analysis yielded an average formulation corresponding to $C_{60}[(CF_2)_5CF_3]_{9.5}H_2$ with traces of chlorine and no iodine (<100 ppm) in the sample (C, 36.85; H, 0.07; F, 61.66; and Cl, 0.50%). Traces of chlorine may arise from the solvent either during reaction or upon work-up. The ultraviolet-visible spectrum in Freon 113 showed a featureless, monotonically decreasing absorption in the range 200 to ~650 nm.
9. Argon was used as a buffer to reduce the kinetic energy of electrons to thermal levels.
10. Results of ^{19}F NMR (283 MHz, 25°C, C_6F_6-CD_2Cl_2) : δ (in parts per million) = −81 (slightly broadened, 3F, CF_3); −96 to −111 [extremely broad, 2F, $CF_2(\alpha)$]; −113 to −118 [broad, 2F, $CF_2(\beta)$]; −121 [broad, 2F, $CF_2(\gamma)$]; −122 [slightly broadened, 2F, CF_2 (δ)]; and −126 [slightly broadened, 2F, $CF_2(\varepsilon)$]. The assignments refer to the position on the perfluoroalkyl chain: C_{60}-$CF_2(\alpha)$-$CF_2(\beta)$-$CF_2(\gamma)$-$CF_2(\delta)$-$CF_2(\varepsilon)$-CF_3. We assume that the further a CF_2 group is from the C_{60} surface, the sharper the resonance of its fluorines will be. Resonances assigned to CF_2 groups closer to the surface are broad because the material is a mixture of different isomers. There is thus a variety of different local chemical environments for the diastereotopic fluorines of the CF_2 groups closer to the C_{60} surface.
11. D. Griller *et al.*, *J. Am. Chem. Soc.* **103**, 7761 (1981).
12. C. Rüchardt *et al.*, *Angew. Chem. Int. Ed. Engl.* **32**, 584 (1993).
13. The expected product from this mechanism, α,α,α-trifluoro-toluene, was detected by ^{19}F NMR and by gas chromatography–mass spectrometry together with smaller amounts of iodobenzene.
14. S. J. McLain, B. Sauer, L. Firment, *Polym. Prepr. Am. Chem. Soc. Div. Polym. Chem.* **34**, 666 (1993).
15. The equivalence of the two fluorines in the perfluoroethyl adduct can be attributed to the presence of a plane of symmetry and not to fast exchange between different environments because no line-shape effects were observed over a very broad temperature range.
16. In ESR, the activation energies that can be extracted from the analysis of temperature-dependent line-shape effects of the data shown in Fig. 3A are generally less than ~5 kcal/mol.
17. See, for example, D. A. Dixon, *J. Phys. Chem.* **96**, 3698 (1992).
18. F. N. Tebbe *et al.*, *Science* **256**, 822 (1992).
19. With the use of standard Corey-Pauling-Koltun (CPK) models, a CF_3 group viewed along the threefold axis can be inscribed by a circle whose diameter is about 33% larger than the diameter of a bromine atom.
20. The structure shown in Fig. 3 is the result of a molecular mechanics calculation (Insight II Molecular Modeling Software; Biosym Technologies, Inc., San Diego, CA).
21. We thank K. Lykke for helpful contributions, D. Dixon for stimulating discussions, J. Krywko for molecular modeling, B. Sauer for contact-angle measurements, and S. Hill, R. Davis, J. B. Jensen, I. Kregers, and R. McKay for technical assistance. The FTMS work was carried out at the Argonne National Laboratory, Argonne, Illinois. DuPont contribution no. 6577.

24 May 1993; accepted 4 August 1993

Isotopic Evidence for Reduced Productivity in the Glacial Southern Ocean

A. Shemesh, S. A. Macko, C. D. Charles, G. H. Rau

Records of carbon and nitrogen isotopes in biogenic silica and carbon isotopes in planktonic foraminifera from deep-sea sediment cores from the Southern Ocean reveal that the primary production during the last glacial maximum was lower than Holocene productivity. These observations conflict with the hypothesis that the low atmospheric carbon dioxide concentrations were introduced by an increase in the efficiency of the high-latitude biological pump. Instead, different oceanic sectors may have had high glacial productivity, or alternative mechanisms that do not involve the biological pump must be considered as the primary cause of the low glacial atmospheric carbon dioxide concentrations.

Measurements of ancient air trapped in ice (*1–3*) indicate that global atmospheric CO_2 concentrations have changed greatly over the last 130,000 years. These concentrations during the last glacial period were lower by about 80 ppm than concentrations during the Holocene and last interglacial. There is agreement that oceanic processes were primarily responsible for these changes because the oceanic reservoir of CO_2 is about 60 times larger than that for the atmosphere (*4*). One general mechanism that helps to explain observed lower surface-ocean CO_2 concentrations is the enhanced photosynthetic uptake of CO_2 and subsequent removal of organic carbon to the deep ocean. This process is known as the biological pump (*5*). Scenarios to alter the efficiency of the biological pump involve changes in global phosphate extraction, denitrification, the C/P ratio of organic tissues, and the organic and inorganic sedimentary carbon pools. However, these scenarios fail to meet constraints placed by ocean sediments and polar ice records (*6*). The surface water in polar regions is critical for the control of the CO_2 system, because the deep sea interacts directly there with the atmosphere. A series of models (*7–9*) demonstrated that atmospheric CO_2 concentrations could be lowered in concert with the biological consumption of nutrients in polar surface waters. Such decreases could be achieved by (i) an increase in high-latitude productivity, (ii) a decrease in the rate of exchange between deep oceanic and polar surface waters, or (iii) both.

This notion and consistent model results prompted an extensive search in the sedimentary record of the Southern Ocean for evidence of the predicted biogeochemical changes. Attempts to trace changes in surface nutrient concentration were made by the measurement of ^{13}C and Cd/Ca ratios in planktonic foraminifera (*10–11*) and Ge/Si ratios in diatoms (*12*). Opal accumulation rates were used to estimate changes in paleoproductivity of the Southern Ocean (*13, 14*), and bulk sediment $\delta^{15}N$ measurements were used to estimate changes in surface-water nitrate utilization (*15*). Although the results are somewhat in disagreement, none of the above studies support the scenario of high-latitude performed nutrients for the deglacial increase in atmospheric CO_2.

Here we tested further the hypothesized variability in the Southern Ocean biological pump over the last glacial cycle by analyzing organic matter preserved in diatom frustules. Diatoms are the main primary producers south of the present polar front, and therefore geochemical characteristics of the siliceous sediments of the Southern Ocean may provide a direct re-

A. Shemesh, Department of Environmental Sciences and Energy Research, Weizmann Institute of Science, Rehovot 76100 Israel.
S. A. Macko, Department of Environmental Sciences, University of Virginia, Charlottesville, VA 22903.
C. D. Charles, Scripps Institution of Oceanography, University of California, San Diego, La Jolla, CA 92093.
G. H. Rau, Institute of Marine Sciences, University of California, Santa Cruz, CA 95064.